Volume 1 | Number 1 | Jan 2013 | Pages 1–100

ChemComm

Chemical Communications
www.rsc.org/chemcomm

ROYAL SOCIETY OF CHEMISTRY

This is an *Accepted Manuscript*, which has been through the Royal Society of Chemistry peer review process and has been accepted for publication.

Accepted Manuscripts are published online shortly after acceptance, before technical editing, formatting and proof reading. Using this free service, authors can make their results available to the community, in citable form, before we publish the edited article. We will replace this *Accepted Manuscript* with the edited and formatted *Advance Article* as soon as it is available.

You can find more information about *Accepted Manuscripts* in the **Information for Authors**.

Please note that technical editing may introduce minor changes to the text and/or graphics, which may alter content. The journal's standard **Terms & Conditions** and the **Ethical guidelines** still apply. In no event shall the Royal Society of Chemistry be held responsible for any errors or omissions in this *Accepted Manuscript* or any consequences arising from the use of any information it contains.

ChemComm

COMMUNICATION

A facile strategy to three-dimensional Pd@Pt core-shell nanoflowers supported on graphene nanosheets as an enhanced nanoelectrocatalyst for methanol oxidation

Yi Chen, Jia Yang, Ying Yang, Zhiyao Peng, Jinhua Li, Tao Mei, Jianying Wang, Ming Hao, Yalin Chen, Weilai Xiong, Liu Zhang and Xianbao Wang[*]

Here we demonstrate for the first time a water-based surfactant-free synthesis of three-dimensional porous Pd@Pt core-shell nanoflowers on graphene. The obtained Pd@Pt/graphene hybrids exhibited substantially enhanced electrocatalytic activity and stability relative to the commercial Pt/C catalyst originating from this exquisite nanoarchitecture for three-dimensional molecular accessibility and graphene-metal interaction.

Platinum (Pt) is a marvellous catalyst for a wide range of reactions, in particular, both fuel oxidation and oxygen reduction reaction occurring on the interface of electrodes and electrolyte of a proton-exchange membrane (PEM) fuel cell.[1-4] However, the scarcity and sky-rocketing price of Pt have become key barriers for its broad deployment in fuel cells for commercial viability. Therefore, it is highly desirable to develop nanoelectrocatalysts with minimal Pt usage while still displaying superior performance. Specifically, combining Pt with a more abundant metal to generate novel bimetallic nanostructures in the form of alloys[5-7], dendrites[1, 8, 9] or core-shells[10-13] has become the most promising approach to reduce the Pt content as well as improve their intrinsic activity on a mass basis. Since Pd and Pt share the same face-centered cubic structure, together with good miscibility and a minor lattice mismatch of only 0.77%,[14] they can be readily prepared as bimetallic core-shell nanocrystals with a single-crystal structure. Meanwhile, the current price of Pd is only 40% that of Pt, making Pd a superb candidate for the core to help reduce the material cost. In addition, theoretical studies indicate that the combination of Pd and Pt can tailor the electronic d-band center of Pt, which has played a decisive role in bringing enhancement for certain catalytic reactions.[15] Accordingly, by using Pd@Pt core-shell nanocrystals as a catalyst, it is expected that the catalytic performance could be optimized and less Pt is needed in the fuel cell reactions, a goal that has long been sought for commercialization of the fuel cell technology.

Hubei Collaborative Innovation Center for Advanced Organic Chemical Materials, Ministry of Education, Key Laboratory for the Green Preparation and Application of Functional Materials, School of Materials Science and Engineering, Hubei University, Wuhan 430062, PR China. E-mail: wangxb68@aliyun.com; Fax: +86-27-8866-1729; Tel: +86-27-8866-2132

On the other hand, in order to further maximize the activity of Pt and minimize the usage of Pt, it is very necessary to disperse Pt-based nanostructures on proper supports. Featuring the excellent electronic properties, huge surface area and unique graphitized basal plane structure,[16-18] graphene is an ideal substrate to facilitate the nucleation and growth of Pt-based nanocrystals for producing functional hybrid nanostructures, which would not only maximize the availability of nanocatalyst surface area for electron transfer but also provide better mass transport of reactants to the nanocatalyst. However, it was reported that the graphene supported metal nanostructures were commonly obtained by adding graphene during the reducing metal precursors or mixing the nanocrystals with graphene, prior to which the surface of metal nanocrystals and/or graphene sheets is functionalized with additional surfactants or ligands to ensure good bonding between them via covalent or non-covalent interactions.[19-23] Unfortunately, the presence of these agents around nanocrystals or graphene may lead to a decrease of active sites and electrical conductivity, which severely limits their electrocatalytic performance.[1, 24-28] Hence, to fully utilize the extraordinary properties of both graphene and Pt by their composites, it is vital to develop a facile and *in situ* co-chemical reduction approach to load "surface-clean" Pd@Pt nanostructures on graphene.

Herein, for the first time, we demonstrate a water-based surfactantless synthesis of three-dimensional (3D) Pd@Pt core-shell nanoflowers on graphene, which represents a new type of graphene/metal hybrid nanostructures with several crucial advantages. (a) "Surface-clean" single-crystal Pd@Pt nanoflowers were grown onto graphene surfaces with superb monodispersity and homogeneity. (b) The Pd@Pt nanoflower is composed of a Pd interior and porous dendritic Pt shell, which would offer three-dimensional molecular accessibility and thereby dramatically diminish the number of buried nonfunctional precious metal atoms and increase the atomic utilization efficiency. (c) Benefiting from this attractive architecture and unique characteristic, the as-prepared Pd@Pt/graphene hybrids exhibited substantially enhanced electrocatalytic activity and stability toward methanol oxidation relative to the PdPt alloy/graphene, Pt/graphene and commercial Pt/C catalyst.

The preparation strategy for constructing the Pd@Pt nanoflowers supported on graphene is demonstrated in Scheme 1 (the detailed experimental procedure is given in the ESI). They were prepared
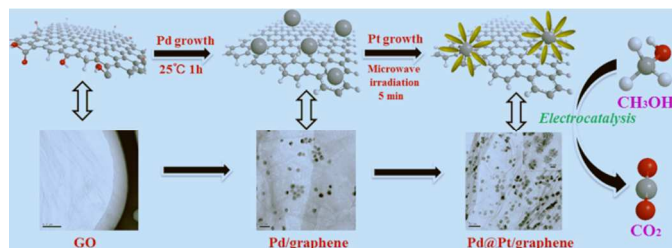
Scheme 1 Schematic presentation for formation of Pd@Pt core-shell nanoflowers onto graphene nanosheets.

using a sequential method. In the first step, we synthesized small Pd nanoparticles uniformly distributed on graphene by reducing graphene oxide (GO) and $PdCl_2$ simultaneously with L-ascorbic acid (AA) in an aqueous solution at room temperature. A transmission electron microscopy (TEM) image of the as-prepared Pd/graphene is shown in Fig. 1a. It is easily discerned that fine nanoparticles of Pd on the surface of graphene nanosheets present an average diameter of around 6.3 nm (Fig. S1a). The high-resolution TEM (HRTEM) image (Fig. 1b) of a single Pd nanocrystal indicates that it is indeed a piece of single crystal with its surface being enclosed mainly by (111) facets. The observed fringes with spacing of 2.25 Å were in agreement with a (111) plane spacing of Pd face-centered cubic (fcc) structure (Fig. S2). These single-crystal Pd nanoparticles supported on graphene nanosheets were then used as seeds to direct the subsequent rapid dendritic growth of Pt for producing 3D porous Pd@Pt core-shell nanoflowers upon the reduction of $H_2PtCl_4 \cdot 6H_2O$ by AA under microwave irradiation for 5 min. It should be noted that the whole preparation strategy has been implemented in an aqueous phase without adding any surfactant or capping agent, thus enabling the obtained product with a very "clean" surface. Typical TEM images at different magnifications (Fig. 1c, d, e) clearly showed that the as-prepared sample had well-dispersed nanoflowers with a completely dendritic shape, demonstrating the high-yield formation. The corresponding EDX spectrum (Fig. S3) showed the peaks corresponding to C, O, Pd and Pt elements, confirming the existence of bimetallic Pd-Pt nanoparticles on the surface of graphene nanosheets. The Pd-Pt bimetallic nanoflowers had an average size of approximately 16.4 nm (Fig. S1b). Well-defined dendritic shells consisted of plentiful of interconnected nanorods of about 3 nm in width. These randomly aggregated nanorods created 3D nanoporous architectures, which were highly favourable for maximizing the accessible surface area for achieving high mass activity of a catalyst. The wide-angle X-ray diffraction (XRD) pattern showed a metallic fcc structure (Fig. S2). In contrast to other core/shell systems, there are no distinct difference in the lattice constants between Pd and Pt fcc crystals. Therefore, we can not distinguish whether a Pd-Pt bimetallic alloy is formed. To make it clear, the elemental distribution of the two metals were further visualized using the corresponding elemental line-scanning analysis. As can be seen in Fig. 1f, Pd and Pt were not uniformly distributed in the nanoflowers, suggesting the formation of Pd@Pt structure consisting of a Pd core and dendritic Pt exterior. The HRTEM image in Fig. 1e showed no obvious grain boundaries between Pd and Pt because of the extremely high lattice match ratio (99.23%)[14]. All of these results demonstrate that, although the core and shell are compositionally different, the crystallographic structure is uniform and coherent over the entire nanoflower, resulting in the formation of an inserted pseudo Pd-Pt alloy heterointerface. Specifically, the spatially and locally separated nanoarms were highly crystallized, and most of the exposed facets were found to be (111) (d-spacing~2.26 Å) in addition to a small fraction of (200) (d-spacing~1.97 Å) (Fig. 1e). This was in agreement with the XRD
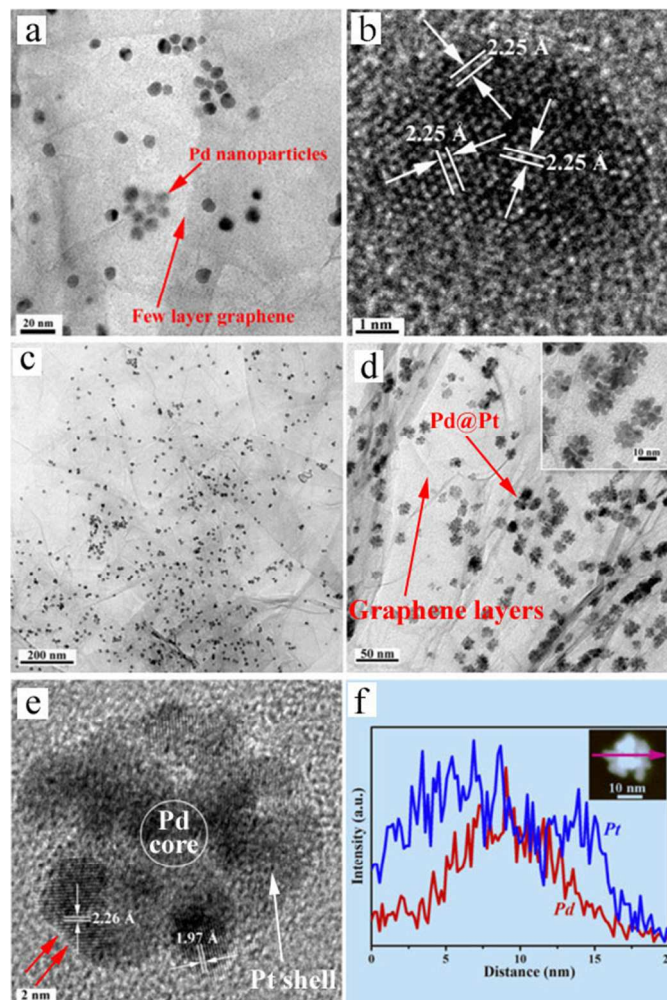

Fig. 1 TEM (a) and HRTEM (b) images of Pd nanoparticles on graphene. Representative TEM (c, d) and HRTEM (e) images of Pd@Pt core-shell nanoflowers on graphene. (f) EDX line-scanning profiles of Pt and Pd across a single Pd@Pt core-shell nanoflower shown in the inset.

profile in Fig. S2. It was noteworthy that abundant atomic steps were successfully exposed on the Pt branch surface (as indicated by the red arrows in Fig. 1e). Such a delicate and unique atomic structure can act as highly active sites for methanol oxidation.[10, 29]

The observed successive dendritic growth of Pt branches on the preformed Pd seeds can probably be attributed to the close matching between the lattice parameter of Pd and Pt and the rapid microwave-assisted reduction of Pt as mediated by an autocatalytic process, which has been used to account for the formation of branched nanostructures of Pt.[1] Interestingly, we also observed branching via autocatalytic reduction of the Pt precursor in the absence of Pd seeds (Fig. S4). However, simultaneous reduction of Pd^{2+} and Pt^{2+} produced foam-like PdPt alloy aggregates on graphene (Fig. S5). Different reduction rates of the metal precursors may play a key role in the different structural evolution of the particles.[30] Furthermore, we attempted to synthesize Pd@Pt nanoflowers with different Pt/Pd molar ratios. When the Pt/Pd molar ratio was increased to 4:1 (Fig. S6a), some irregular and solid particles were produced, because of the weak inducement capacity from the lower Pd content. On the other hand, the obtained product had a lower degree of porosity as the Pt/Pd molar ratio was reduced to 1:4 (Fig. S6c), which was unfavorable for dendrite growth. These results suggest that appropriate Pt/Pd ratio is critical for producing Pd@Pt core-
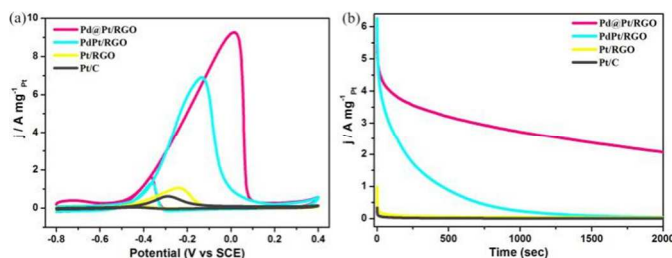
Fig. 2 (a) Cyclic voltammograms and (b) chronoamperometric curves for methanol oxidation reaction catalysed by graphene/Pd@Pt nanoflowers (shown in Fig. 1c, d, e), graphene/PdPt alloy nanofoams (shown in Fig. S5), graphene/branched Pt nanoparticles (shown in Fig. S4) and commercial Pt/C (shown in Fig. S7) in an aqueous solution containing 1 M KOH and 1 M CH_3OH. The Cyclic voltammograms curves were recorded at a scan rate of 50 mV s^{-1} and the chronoamperometric curves were recorded at -0.2V.

shell nanoflowers with an open-framework structure. It must be emphasized that our current understanding of these syntheses is still far from being able to present atomistic details for the evolution pathways that the precursor compound may take to form metal atoms, nuclei, and then well-defined nanoflowers.[31, 32] We believe that salient experiment and theoretical advances in the future would endow us with the ability to fully reveal the details involved in the growth process.

Inspired by their attractive structure and unique characteristic, the graphene supported Pd@Pt nanoflowers were tested as nanoelectrocatalysts for studying their catalytic activity towards the oxidation of methanol (Fig. 2a). To make a comparison, the electrocatalytic activity of PdPt alloy/graphene (shown in Fig. S5), Pt/graphene (shown in Fig. S4) and commercial Pt/C (shown in Fig. S7) was also examined. The currents were normalized to the loading amount of Pt in order to compare the mass activity of different catalysts. As seen in Fig. 2a, the graphene supported Pd@Pt core-shell nanoflowers exhibited the highest mass activity, with a peak current of 9.23 A mg$^{-1}_{Pt}$, which was around 1.3, 8.9, and 14.2 times greater than that of PdPt/graphene (6.89 A mg$^{-1}_{Pt}$), Pt/graphene (1.04 A mg$^{-1}_{pt}$) and commercial Pt/C (0.65 A mg$^{-1}_{Pt}$) catalyst, respectively. If the total amount of metal was taken into account, the mass activity of the graphene/Pd@Pt nanoflowers (5.18 A mg$^{-1}_{Pt+Pd}$) was still the highest of the different catalysts, which was approximately 8.0 times greater than that of the Pt/C catalyst (Fig. S8). It was further noted that the catalytic activity of Pd@Pt nanoflowers on graphene was almost 2.6 times higher than that of recent state-of-the-art PdPt alloy nanowires.[33] In addition, the onset potential of Pd@Pt/graphene was more negative than those of other catalysts, which also indicates substantially enhanced electrocatalytic activity of the graphene/Pd@Pt nanoflowers toward methanol oxidation. It is worthwhile to say that the much improved electrocatalytic activity of Pd@Pt core-shell nanoflowers on graphene could be ascribed to 3 major factors: (a) The graphene/Pd@Pt nanoflowers are very "clean" because of the surfactant-free formation process, allowing them to fully expose active sites for methanol oxidation; (b) The Pd@Pt nanoflower consists of a Pd interior and porous dendritic Pt shell, owning "smart" geometric and electronic structures, which would offer three-dimensional molecular accessibility, thus dramatically increasing the atomic utilization efficiency; (c) Excellent monodispersity and homogeneity of Pd@Pt nanoflowers loaded on graphene nanosheets with high surface area should be also emphasized.

Durability is one of the critical factors for a practical catalyst. To evaluate the stability of the catalysts, chronoamperometric measurements were performed at -0.2 V for 2000 s in an aqueous solution containing 1 M KOH and 1 M CH_3OH. It can be clearly

seen from Fig. 2b that the graphene/Pd@Pt nanoflowers electrode showed much slower attenuation than other catalysts during the entire testing time. Our 3D Pd@Pt core-shell nanoflowers with spatially and locally nanosegregated Pt nanoarms favoured the drastic suppression of the activity loss derived from the undesirable agglomeration of Pt active sites. As mentioned above, the atoms of Pd and Pt are highly miscible and the Pd atoms in the Pd-rich core coherently match with the exterior Pt-rich shell, resulting in the formation of an inserted pseudo Pd-Pt alloy heterointerface (Fig 1e), of which the Pd (as an oxophilic element) can enhance the removal of adsorbed CO on neighbouring Pt atoms by adsorbing oxygen-containing species, enabling enhancement in both activity and durability.[10, 29]

In summary, we have developed a facile, solution-phase, and surfactantless synthesis of 3D Pd@Pt core-shell nanoflowers supported on graphene nanosheets with superb monodispersity and homogeneity. This pioneering approach enables us to synthesize "surface-clean" multimetallic nanocrystals with sophisticated nanoarchitectures, which can not be easily achieved otherwise. The key factor in the proposed method should be attributed to the rapid Pt growth as mediated by the microwave irradiation, resulting in the porous dendritic architecture. Since they have three-dimensional electrocatalytic surfaces, our graphene/Pd@Pt hybrids are highly active catalysts for methanol oxidation reaction relative to other Pt materials. This simple, straightforward and general methodology should be highly inspiring for routinely producing new metallic core-shell nanostructures with large surface areas.

Notes and references

1 B. Lim, M. J. Jiang, P. H. C. Camargo, E. C. Cho, J. Tao, X. M. Lu, Y. M. Zhu and Y. N. Xia, *Science*, 2009, **324**, 1302.
2 C. Chen, Y. J. Kang, Z. Y. Huo, Z. W. Zhu, W. Y. Huang, H. L. Xin, J. D. Synder, D. G. Li, J. A. Herron, M. Mavrikakis, M. F. Chi, K. L. More, Y. D. Li, N. M. Markovic, G. A. Somorjai, P. D. Yang and V. R. Stamenkovic, *Science*, 2014, **343**, 1339.
3 M. Liu, R. Z. Zhang and W. Chen, *Chem. Rev.*, 2014, **114**, 5117.
4 H. Li, J. Wang, M. Liu, H. Wang, P. Su, J. Wu and J. Li, *Nano Res.*, 2014, **7**, 1007.
5 L. H. Li, Y. Wu, J. Lu, C. Y. Nan and Y. D. Li, *Chem. Comm.*, 2013, **49**, 7486.
6 V. R. Stamenkovic, B. Fowler, B. S. Mun, G. Wang, P. N. Ross, C. A. Lucas and N. M. Markovic, *Science*, 2007, **315**, 493.
7 C. H. Cui, L. Gan, M. Heggen, S. Rudi and P. Strasser, *Nat. Mater.*, 2013, **12**, 765.
8 L. Wang, Y. Nemoto and Y. Yamauchi, *J. Am. Chem. Soc.*, 2011, **133**, 9674.
9 Y. J. Li, W. C. Ding, M. R. Li, H. B. Xia, D. Y. Wang and X. T. Tao, *J. Mater. Chem. A*, 2015, **3**, 368.
10 H. A. Esfahani, M. Imura, Y. Yamauchi, *Angew. Chem. Int. Ed.*, 2013, **52**, 13611.
11 D. L. Wang, H. L. Xin, R. Hovden, H. S. Wang, Y. C. Yu, D. A. Muller, F. J. DiSalvo and H. D. Abruna, *Nat. Mater.*, 2013, **12**, 81.
12 J. Zhu, M. Xiao, K. Li, C. Liu and W. Xing, *Chem. Comm.*, 2015, **51**, 3215.
13 F. Zheng, W.-T. Wong and K.-F. Yung, *Nano Res.*, 2014, **7**, 410.
14 H. Zhang, M. S. Jin and Y. N. Xia, *Chem. Soc. Rev.*, 2012, **41**, 8035.
15 S. F. Xie, S. I. Choi, N. Lu, L. T. Roling, J. A. Herron, L. Zhang, J. Park, J. G. Wang, M. J. Kim, Z. X. Xie, M. Mavrikakis and Y. N. Xia, *Nano lett.*, 2014, **14**, 3570.
16 Y. Chen, J. Li, T. Mei, X. G. Hu, D. W. Liu, J. C. Wang, M. Hao, J. H. Li, J. Y. Wang and X. B. Wang, *J. Mater. Chem. A*, 2014, **2**, 20714.

17 X. Huang, C. L. Tan, Z. Y. Yin and H. Zhang, *Adv. Mater.*, 2014, **26**, 2185.
18 S. C. Sahu, A. K. Samantara, A. Dash, R. R. Juluri, R. K. Sahu, B. K. Mishra and B. K. Jena, *Nano Res.*, 2013, **6**, 635.
19 S. J. Guo, S. J. Dong and E. K. Wang, *ACS Nano*, 2010, **4**, 547.
20 S. J. Guo and S. H. Sun, *J. Am. Chem. Soc.*, 2012, **134**, 2492.
21 C. G. Hu, H. H. Cheng, Y. Zhao, Y. Hu, Y. Liu, L. M. Dai and L. T. Qu, *Adv. Mater.*, 2012, **24**, 5493.
22 X. Huang, S. Li, S. Wu, Y. Huang, F. Boey, C. L. Gan and H. Zhang, *Adv. Mater.*, 2012, **24**, 979.
23 Y. J. Li, Y. J. Li, E. B. Zhu, T. McLouth, C.-Y. Chiu, X. Q. Huang and Y. Huang, *J. Am. Chem. Soc.*, 2012, **134**, 12326.
24 X. M. Chen, G. H. Wu, J. M. Chen, X. Chen, Z. X. Xie and X. R. Wang, *J. Am. Chem. Soc.*, 2011, **133**, 3693.
25 J. Mao, Y. Liu, Z. Chen, D. Wang and Y. Li, *Chem. Comm.,* 2014, **50**, 4588
26 M. Jiang, B. Lim, J. Tao, P. H. C. Camargo, C. Ma, Y. Zhu and Y. Xia, *Nanoscale*, 2010, **2**, 2406.
27 K. Sasaki, H. Naohara, Y. Cai, Y. M. Choi, P. Liu, M. B. Vukmirovic, J. X. Wang and R. R. Adzic, *Angew. Chem. Int. Ed.* 2010, **49**, 8602.
28 H. Zhang, M. Jin, J. Wang, M. J. Kim, D. Yang and Y. Xia, *J. Am. Chem. Soc.*, 2011, **133**, 10422.
29 L. Wang and Y. Yamauchi, *J. Am. Chem. Soc.*, 2013, **135**, 16762.
30 Y. Kim, Y. Noh, E. J. Lim, S. Lee, S. M. Choi and W. B. Kim, *J. Mater. Chem. A*, 2014, **2**, 6976.
31 Y. Wu, D. S. Wang and Y. D. Li, *Chem. Soc. Rev.*, 2014, **43**, 2112
32 Y. Xia, Y. Xiong, B. Lim and S. E. Skrabalak, *Angew. Chem. Int. Ed*, 2009, **48**, 60.
33 C. Zhu, S. Guo and S. Dong, *Adv. Mater.*, 2012, **24**, 2326.

ChemComm Accepted Manuscript